Journal of Thermal Biology 84 (2019) 16–25

Contents lists available at ScienceDirect

Journal of Thermal Biology

journal homepage: www.elsevier.com/locate/jtherbio

Identifying heat source intensity in treatment of cancerous tumor using therapy based on local hyperthermia – The Trefftz method approachs

K. Grysa, A. Maciąg*

Kielce University of Technology, Al. Tysiąclecia Państwa Polskiego 7, 25-314, Kielce, Poland

ARTICLE INFO

Keywords:
Non-fourier model
Perfusion
Bioheat
Tumor
Source identification
Trefftz function
Inverse problem

ABSTRACT

The presented study considers the equation of hyperbolic conduction of heat with perfusion in order to identify such intensity of spatial heat source that will lead to hyperthermia of a cancerous tumor placed in healthy tissue. The tumor is assumed to be in the form of a sphere with a small radius. In order that the determined intensity of the heat source does not damage healthy tissue, different temperature distributions as a function of time are anticipated at the tumor's border. The mathematical tools used are based on the Trefftz method. The results are presented in the form of numbers and graphs illustrating the intensity of the identified heat source and matching the obtained temperature distributions in the tumor to the predicted ones.

1. Introduction

Cancer, the main cause of death in developed countries, is the second leading cause of death in developing countries (Siegel et al., 2013). Solid tumors account for 85% of human cancers (Soltani and Chen, 2012). Hyperthermia treatment is recognized as the fourth adjunct cancer therapy technique following surgery, chemotherapy, and radiation techniques. In hyperthermia, the tumor cells will be overheated to a therapeutic value, typically 40–45 °C to damage or kill the cancer cells and affect the metastases (Hall and Roizin-Towle, 1984; Field, 1987; Habash et al., 2006). It is a type of cancer treatment in which body tissue is exposed to high temperatures, using external and/or internal heating devices.

In numerous articles, the authors investigated thermal behavior inside a tumor found in healthy tissue. In the study investigating the effect of tumor on the thermal behavior inside the skin tissue (Fu et al., 2017), the authors apply the method of approximating particular solutions to simulate the tumor in 3-dimensions (3D) for solving the Pennes' bioheat equation. Hafid and Lacroix (2017), also considered the Pennes' equation. In their paper the Levenberg-Marquardt Method combined with the Broyden Method (the Jacobian is updated using the Broyden update formula) has been used to predict the time-varying freezing front and the temperature distribution of tumors during cryosurgery. The Markov chain Monte Carlo method for the estimation of parameters appearing in the Pennes' equation is used in order to detect skin tumors by using surface temperature measurements. (Rojczyk et al., 2015). Luna et al., 2014, considering the Pennes' equation for estimating thermo-physical and geometrical parameters of very small hypothetical skin tumors (with the use a surface temperature profile), used a numerical procedure based on the Boundary Element Method coupled with the Simulated Annealing technique. Khanday et al., 2013, studied the hyperthermic approach to damaging tumor cells by introducing a circular magnetic element in the region under consideration. The heat source of constant density of radius r_0 at the center was used to solve the Pennes' bioheat equation analytically. LiuLin C, 2010, studied the non-Fourier bioheat equation and obtained solutions to the hyperbolic bio-heat equation with the space-dependent source term in the spherical coordinate system. In this paper, the Laplace transform technique was applied whereas the space domain was divided into several sub-space domains. The thermal wave model is used to predict the temperature excess occurring in a two-layer concentric spherical tissue when the tumor is heated by magnetic nanoparticles playing the role of localized heat sources. A similar method was used to solve various problems related to non-Fourier heat transfer problems (Liu, 2007a, 2007b, 2008).

An ideal hyperthermia treatment should destroy the tumor cells without damaging the surrounding healthy tissue. The greater problem is to obtain a reliable temperature value in the hyperthermia region. In the present paper, the intensity of the heat source heating the tumor in order to kill the cancer cells is identified. This kind of issue belongs to the so-called inverse problems. As in the article of LiuLin C, 2010, the non-Fourier bioheat equation in a two-layer concentric spherical region is used to predict the thermal behavior during the tumor hyperthermia treatment. As a tool to solve the problem, the method of approximating

* Corresponding author.
E-mail address: maciag@tu.kielce.pl (A. Maciąg).

https://doi.org/10.1016/j.jtherbio.2019.06.004
Received 15 January 2019; Received in revised form 18 April 2019; Accepted 2 June 2019
Available online 04 June 2019

Nomenclature

ai	coefficients, Eq. (28)
A	in variables separation, Eq. (24)
$b_i(r, t)$	monomials $r^k t^m$, $k, m \geq 0$
B	in variables separation, Eq. (24)
c	specific heat of tissue, J/(kg K)
cb	specific heat of blood, J/(kg K)
cn	a coefficient in linear combination of T-functions, Eq. (25)
Fn	n-th T-function, Eq. (27)
$g(\Phi, t)$	a function in Eq. (9)
G	$= \tau\beta^2 + 1$, dimensionless
i	a subscript, =1 for tumor, =2 outside
I	objective functional , Eq. (41)
L	operator, Eq. (29)
L-1	inverse operator, Eq. (31)
L	Laplace transform designation
p	a parameter, Eq. (24), 1/s
q	heat flux, W/m2
Qm	$= r/(c\bar{Q}_m)$, mK/s
Qr	$= r/(c\bar{Q}_r)$, mK/s
$\bar{Q}$m	metabolic heat generation, W/m3
$\bar{Q}$r	spatial heating source, W/m3
r	spatial coordinate, m
R	radius of the tumor, m
$\mathbb{R}$	set of real numbers
t	time, s
T	temperature, K
Tb	arterial temperature, K
Tcr	critical temperature, K
Vkl	T-functions, k=1,2,3,4, l=0,1,…
wb	perfusion rate of blood, m3/s/m3

Greek letters

β^2	$= (\omega_b \rho_b c_b)/(c, 1/s)$
Φ	a parameter, Eq. (9)
Γi	ith generating functions, i=1,2,3,4
$\varkappa$	$= \frac{\lambda}{\rho c}$, thermal diffusivity, m2/s
λ	thermal conductivity, W/mK
ρ	density, kg/m3
ρb	density off blood, kg/m3
θ	$= r(T - T_b)$, mK
θ^b	approximate general solution, Eq. (27)
$\theta_1^P(r, t)$	particular solution, Eq. (33)
$\theta_2^P(r, t)$	particular solution, Eq. (32)
τ	relaxation time, s
ζ	$= \frac{q}{\lambda}$, K/m

Subscripts

1	applies to tumor
2	applies to healthy tissue

a solution of the problem with a linear combination of Trefftz functions (T-functions) has been used. An approximate solution to the problem is obtained by means of minimizing the functional which describes the mean square error of the conditions' approximation and anticipated internal temperature responses by this linear combination.

The Trefftz method is widely described in many papers and monographs, (Li et al., 2008; Kołodziej and Zieliński, 2009; Grysa, 2010; Ciałkowski and Grysa, 2010; Grysa et al., 2014). The T-functions for a linear partial differential equation can usually be obtained by the method of variables separation. Expanding the solution(s), called generating function(s), into power series with respect to the parameter(s) resulting from the method of variable separation one arrives to T-functions. The T-functions, determined for a linear differential equation describing the physical problem under consideration, satisfy this equation identically and, moreover, they form a complete system and are square integrable. (A system of square integrable functions will be complete if, and only if, any square integrable function on the interval [a, b] can be approximated in the mean to any desired degree of accuracy by a linear combination of functions from the system.)

The article presents a mathematical model of choosing such a method of heating a cancerous tumor to lead to its hyperthermia. The tumor has been modeled as a sphere with a given radius, and the tissue of its healthy environment as the larger sphere in which the tumor is located. It was assumed that the radius of the sphere describing the surroundings is large enough that the temperature of its outer boundary is equal to the temperature of arterial blood. In order to destroy the tumor, nanoparticles of the magnetic fluid are injected into it, which are then dispersed randomly inside the tumor. The temperature of these molecules can be regulated, thus creating a spatial source of heat in the tumor. The aim of the paper is to determine the intensity of the heat source thus created to destroy the tumor without destroying the healthy tissue in the environment. This kind of issues belongs to the class of inverse problems.

To solve the problem, the temperature field in the tumor and in the surrounding tissue have been modeled with the use of non-Fourier bioheat equation (wave equation) with perfusion. To determine the approximate solution to the problem, i.e. the temperature field in the tumor and in the surrounding healthy tissue as well as the intensity of the spatial heat source in the tumor, the Trefftz method was used. At the interface between the cancerous tumor and the healthy tissue, it was necessary to establish conditions that would guarantee that the tumor would be destroyed and healthy tissue would not. Two variants of anticipated temperature changes in time on the border of tumor have been considered. In addition, different shapes of the function describing the heat sources were adopted.

The temperature field in the tumor and in healthy tissue have been described in an approximate way by linear combinations of T-functions. By minimizing the approximation error of the initial and marginal conditions in the tumor, in the surrounding healthy tissue and on the interface of healthy tissue and tumor, both the temperature field in the tumor and in surrounding tissue as well as the intensity of the spatial source in the tumor were determined in the mean square sense.

This made it possible to estimate the intensity of the spatial heat source in the tumor, check the correctness of the expected temperature distribution at the interface between the tumor and healthy tissue, and check which function describing the heat sources in the tumor is the most correct, comparing the results with those obtained in a similar problem cited in the literature.

2. Non-Fourier bioheat equation

A small tumor is usually regarded as a solid sphere with the radius R, (Andra et al., 1999; Bagaria and Johnson, 2005; Maenosono and Saita, 2006; LiuLin C, 2010). The tumor is heated. The temperature distribution in the tumor ($0 \leq r \leq R$) and inside the healthy tissues ($R \leq r < \infty$) is a function of the distance $r$from the center of the sphere and time t.

The linearized relationship between the heat flux vector and the thermal disturbance in the thermal wave model is described as:

$$q + \tau\frac{\partial q}{\partial t} = -\lambda\frac{\partial T}{\partial r} \tag{1}$$

where T is the temperature, λ the heat conductivity, q the heat flux, t the time, and r the space variable, (Cattaneo, 1958; Vernotte, 1958; Weymann, 1967). The wave model is also called the single-phase lag model (abbr. SPL). It is a model that introduces the concept of the relaxation time, τ, as the build-up time for the onset of thermal flux after a temperature gradient is suddenly imposed on the sample.

The local energy balance in the case considered in the paper (one-dimensional problem, spherical coordinates) has the form

$$\rho c\frac{\partial T}{\partial t} = -\frac{\partial q}{\partial r} - \frac{2}{r}q + w_b\rho_b c_b(T_b - T) + \bar{Q}_m + \bar{Q}_r \tag{2}$$

where ρ and c denote density ad specific heat in two regions (in the healthy tissue and in the tumor). ρ_b, c_b, and w_b, respectively, are the density, specific heat, and perfusion rate of blood. $\bar{Q}_m$ is the metabolic heat generation and $\bar{Q}_r$ stands for spatial heating source; both are assumed to be constant. T_b is the arterial blood temperature.

Substituting Eq. (1) into the energy conservation Eq. (2) and assuming $\lambda = \text{const}$ leads to the equation as follows

$$\lambda\frac{1}{r^2}\frac{\partial}{\partial r}\left(r^2\frac{\partial T}{\partial r}\right) = \rho c\left(\frac{\partial T}{\partial t} + \tau\frac{\partial^2 T}{\partial t^2}\right) + \omega_b\rho_b c_b(T_b - T) - \bar{Q}_m - \bar{Q}_r + \tau\omega_b\rho_b c_b\frac{\partial T}{\partial t} \tag{3}$$

It is assumed that at a distance equal to or greater than 5R the temperature of healthy tissue is equal to T_b. For convenience of analysis, new functions, θ and ζ, are defined as

$$\theta = r(T - T_b)[mK] \text{ and } \zeta = \frac{q}{\lambda}, [K/m] \tag{4}$$

2.1. After multiplying by $\frac{r}{\lambda}$, Eq. (3) takes the form

$$\frac{\partial^2\theta}{\partial r^2} = \frac{\rho c}{\lambda}\left(\frac{\partial\theta}{\partial t} + \tau\frac{\partial^2\theta}{\partial t^2}\right) + \frac{\omega_b\rho_b c_b}{\lambda}\theta - \frac{r}{\lambda}(\bar{Q}_m + \bar{Q}_r) + \frac{\tau\omega_b\rho_b c_b}{\lambda}\frac{\partial\theta}{\partial t}$$

or

$$\frac{\lambda}{\rho c}\frac{\partial^2\theta}{\partial r^2} - \frac{\omega_b\rho_b c_b}{\rho c}\theta = \tau\frac{\partial^2\theta}{\partial t^2} + \left(\frac{\tau\omega_b\rho_b c_b}{\rho c} + 1\right)\frac{\partial\theta}{\partial t} - \frac{r}{\rho c}(\bar{Q}_m + \bar{Q}_r) \tag{5}$$

2.2. Let us introduce the quantities

$$\varkappa = \frac{\lambda}{\rho c},\ \beta^2 = \frac{\omega_b\rho_b c_b}{\rho c},\ G = \tau\beta^2 + 1 \tag{6}$$

and denote

$$Q_m = \frac{r}{\rho c}\bar{Q}_m \text{ and } Q_r = \frac{r}{\rho c}\bar{Q}_r[mK/s] \tag{7}$$

Eq. (5) will be considered separately for $0 \le r \le R$ (the region in which coefficients and functions will be marked with subscript 1) and separately for $R < r \le 5R$(subscript 2). Then, with (6) and (7) one arrives at the following form of Eq. (5)

$$\varkappa_i\frac{\partial^2\theta_i}{\partial r^2} - \beta_i^2\theta_i - \tau_i\frac{\partial^2\theta_i}{\partial t^2} - G_i\frac{\partial\theta_i}{\partial t} = -Q_{mi} - Q_{ri},\ i = 1,2 \tag{8}$$

Thus, in the following considerations, two equations will be solved in an approximate way. equation (8) for i = 1 describes the temperature in the tumor for $0 \le r \le R$. The same equation for $i = 2$ describes the temperature in healthy tissue, for $R < r \le 5R$. All coefficients with indicator 1 will refer to the tumor and describe its thermomechanical properties, while coefficients with indicator 2 refer to healthy tissue and its properties. Note that the intensity of the spatial heat source in the tumor, Q_{r1}, is the unknown (sought after) function of the spatial variable and time. The intensity of the spatial heat source in healthy tissue, Q_{r2}, is zero. However, it is assumed that the intensity of the metabolic heat source in the tumor and in healthy tissue is constant, but has a different value in the tumor than in healthy tissue. The figures are presented in the "*Results and Discussion*" section.

equation (8) for the tumor and for healthy tissue will be solved in an approximate way using the Trefftz method and the inverse operators method. Both methods are described in the following sections. The next section presents a mathematical description of the initial conditions in the tumor and in healthy tissue, the assumed form of temperature distribution on the interface between the tumor and healthy tissue and the conditions on the outer boundary of the considered area, i.e. for $r = R$.

2.3. Formulation of the problem

The intensity of the spatial heat source leading to necrotize the tumor cells, Q_r, is an unknown. In magnetic fluid hyperthermia, magnetic particles are injected into the center of the tumor accumulating mainly in its center and diffusing inside in a random way. The anticipated internal temperature response for $r = R$is assumed in the form

$$\theta_1(R, t) = \theta_2(R, t) = R(T_{cr} - T_b)g(\Phi, t) \tag{9}$$

where the parameter Φ controls the heating speed and T_{cr}denotes a critical temperature above which the tumor is destroyed. The function $g(\Phi, t)$describes the assumed temperature distribution in time for $0 < t \le 250$ s:

1) $g(\Phi, t) = \frac{\Phi t}{1 + \Phi t}$ for Φ=0.005, 0.01, 0.015 ;
2) $g(\Phi, t) = 0.004t$ for $t \in (0,\ 250)$.

The degree of matching the course of the identified temperature in time for $r = R$will indicate which of the anticipated distributions is more likely. The critical temperature should not be lower than 42,5°C so that the cancer cells have a higher chance of dying. The maximum efficiency of the spatial heating source, Q_{r1}, should be so high as to necrotize the undesirable tissue. The spatial heating source in the healthy tissue, Q_{r2}, is assumed to be equal to zero.

Let us go back for a while to Eq. (3) describing the temperature field in the tumor and in healthy tissue. Initial and boundary conditions will be defined for both areas. The following assumptions should be fulfilled: the temperature in the middle of the tumor should have a limited value, the temperature on the outer boundary of the healthy tissue should be equal to the arterial blood temperature, the initial temperature in the whole area (just before the onset of heating of the magnetic nanoparticles in the tumor) should also be equal to the arterial blood temperature, and moreover at the tumor border the temperature and heat flow should be the same on both sides of the border (in healthy tissue and in the tumor). The mathematical form of these conditions is as follows:

$$T_1(0, t) = \text{finite}, \tag{10}$$

$$T_2(5R, t) = T_b \tag{11}$$

$$T_i(r,\ 0) = T_b,\ i = 1,2 \tag{12}$$

$$\left.\frac{\partial T_i}{\partial t}\right|_{(r,0)} = 0,\ i = 1,2 \tag{13}$$

$$T_1(R, t) = T_2(R, t) \tag{14}$$

$$q_1(R, t) = q_2(R, t) \tag{15}$$

According to formula (4), the temperature difference, $T - T_b$, is equal to $\frac{\theta}{r}$, the value being indeterminate for $r = 0$.Therefore, the value of the transient temperature at the center, $T_1(0, t)$, is transformed using the L'Hospital's rule as

$$T_1(0,\,t) = \lim_{r\to 0}\frac{\theta_1}{r} + T_b = \left.\frac{\partial\theta_1}{\partial r}\right|_{(0,t)} + T_b \tag{16}$$

comp. LiuLin C, 2010. Because $\theta = r(T - T_b)$, therefore in the tumor

$$\theta_1(0,\,t) = 0 \tag{17}$$

Due to the substitution (4) , (6) and (9) the conditions above will be accepted for Eq. (8) as follows:

$$\theta_2(5R,\,t) = 0 \tag{18}$$

$$\theta_i(r,\ 0) = 0,\ i = 1{,}2, \tag{19}$$

$$\left.\frac{\partial\theta_i}{\partial t}\right|_{(r,0)} = 0,\ i = 1{,}2, \tag{20}$$

$$\theta_1(R,\,t) = \theta_2(R,\,t) = R(T_{cr} - T_b)g(\Phi,\,t) \tag{21}$$

$$\lambda_1\zeta_1(R,\,t) = \lambda_2\zeta_2(R,\,t) \tag{22}$$

3. Method of solution

In order to solve Eq. (8) with unknown spatial heating source, Q_r, one has to find a general solution of the homogeneous equation

$$\varkappa_i\frac{\partial^2\theta_i}{\partial r^2} - \tau_i\frac{\partial^2\theta_i}{\partial t^2} - G_i\frac{\partial\theta_i}{\partial t} - \beta_i^2\theta_i = 0,\ i = 1{,}2 \tag{23}$$

For $i = 1$ Eq. (23) describes the temperature in the tumor; for $i = 2$ – in healthy tissue, The next step is to anticipate the form of the spatial heating source as a polynomial and show the way to obtain a particular solution for Eq. (8).

In order to find an approximate form of the general solution of Eq. (23), the Trefftz functions (T-functions) have to be derived for the equation. Since the thermo-physical properties of the tumor and of the surrounding tissue are different, the T-functions for each region will have the same form, but will be determined by other dimensionless parameters. The approximate general solution, θ^b, is assumed to have a form of a linear combination of T-functions. The T-functions are derived in the "*Trefftz functions*" section.

The way of finding the particular solution for Eq. (8) is described in the "*Inverse operator for* Eq. (23)" section.

Knowledge of the T-functions and the anticipated polynomial form of the spatial heat source is sufficient to formulate the problem of minimizing the objective functional that describes the mean square error of fulfilling the initial and boundary conditions by the assumed form of the solution, i.e. the sum of the general and the particular solutions of Eq. (8) for $i = 1{,}2$. The functional is presented in the "*The objective functional*" section. Minimizing the objective functional with respect to the coefficients of the a linear combination of T-functions describing the general solution leads to a system of algebraic equations for coefficients of the T-function linear combination. The matrix of the system is ill-conditioned. However, using the so-called "multiple-scale polynomial Trefftz method" significantly improves the condition number of the matrix without losing the accuracy of calculations, (Liu et al., 2016).

The heat flux has to be expressed by temperature. It is done in the "*Heat flux expressed by temperature*" section.

4. Trefftz functions

T-functions for Eq. (23) can be obtained by solving the equation by means of variables separation. Let $\theta(r,\,t) = A(r)B(t)$. Then it's easy to get two equations with the $p \in \mathbb{R}$parameter:

$$\varkappa\frac{d^2A}{dr^2} - (\beta^2 + p)A = 0 \quad \text{and} \quad \tau\frac{d^2B}{dt^2} + G\frac{dB}{dt} - pB = 0, \tag{24}$$

Next, four so-called generating functions are obtained, resulting from solutions for the function $\theta(r,\,t)$:

$$\begin{aligned}
\Gamma_1(r,\,t) &= exp\left[r\sqrt{\frac{\beta^2+p}{\varkappa}} + \frac{t}{2\tau}(-G + \sqrt{G^2+4p\tau})\right],\\
\Gamma_2(r,\,t) &= exp\left[-r\sqrt{\frac{\beta^2+p}{\varkappa}} + \frac{t}{2\tau}(-G + \sqrt{G^2+4p\tau})\right],\\
\Gamma_3(r,\,t) &= exp\left[r\sqrt{\frac{\beta^2+p}{\varkappa}} + \frac{t}{2\tau}(-G - \sqrt{G^2+4p\tau})\right],\\
\Gamma_4(r,\,t) &= exp\left[-r\sqrt{\frac{\beta^2+p}{\varkappa}} + \frac{t}{2\tau}(-G - \sqrt{G^2+4p\tau})\right],
\end{aligned} \tag{25}$$

Expanding each one of the functions Γ_i, $i = 1{,}2{,}3{,}4$, into the Taylor series with respect to parameter p and then applying the formula

$$V_{ik} = \left.\frac{1}{k!}\frac{d^k\Gamma_i}{dp^k}\right|_{p=0}$$

leads to T-functions as follows:

$$\begin{aligned}
V_{10} &= e^{r\frac{\beta}{\sqrt{\varkappa}}},\ V_{11} = e^{r\frac{\beta}{\sqrt{\varkappa}}}\left(\frac{r}{2\beta} + \frac{t}{G}\right),\ V_{12}\\
&= e^{r\frac{\beta}{\sqrt{\varkappa}}}\left(\frac{r^2}{8\beta^2} - \frac{r}{8\beta^3} + \frac{tr}{2\beta G} - \frac{\tau t}{G^3} + \frac{t^2}{2G^2}\right),\ V_{13}\\
&= e^{r\frac{\beta}{\sqrt{\varkappa}}}\left[\frac{r^3}{48\beta^3} - \frac{r^2}{16\beta^4} + \frac{r}{16\beta^5} - (G^2+4\tau\beta^2)\frac{tr}{8\beta^3G^3} + \frac{tr^2}{8\beta^2G} + \frac{t^2r}{4\beta G^2}\right.\\
&\quad \left. + \frac{t^3}{6G^3} - \frac{\tau t^2}{G^4} + \frac{2\tau^2 t}{G^5}\right],\\
V_{20} &= e^{-r\frac{\beta}{\sqrt{\varkappa}}},\ V_{21} = e^{-r\frac{\beta}{\sqrt{\varkappa}}}\left(-\frac{r}{2\beta} + \frac{t}{G}\right),\ V_{22}\\
&= e^{-r\frac{\beta}{\sqrt{\varkappa}}}\left(\frac{r^2}{8\beta^2} + \frac{r}{8\beta^3} - \frac{tr}{2\beta G} - \frac{\tau t}{G^3} + \frac{t^2}{2G^2}\right),\\
V_{23}&\\
&= e^{-r\frac{\beta}{\sqrt{\varkappa}}}\left[-\frac{r^3}{48\beta^3} - \frac{r^2}{16\beta^4} - \frac{r}{16\beta^5} + (G^2+4\tau\beta^2)\frac{tr}{8\beta^3G^3} + \frac{tr^2}{8\beta^2G}\right.\\
&\quad \left. - \frac{t^2r}{4\beta G^2} + \frac{t^3}{6G^3} - \frac{\tau t^2}{G^4} + \frac{2\tau^2 t}{G^5}\right],\\
V_{30} &= e^{r\frac{\beta}{\sqrt{\varkappa}} - \frac{Gt}{\tau}},\ V_{31} = e^{r\frac{\beta}{\sqrt{\varkappa}} - \frac{Gt}{\tau}}\left(\frac{r}{2\beta} - \frac{t}{G}\right),\ V_{32}\\
&= e^{r\frac{\beta}{\sqrt{\varkappa}} - \frac{Gt}{\tau}}\left(\frac{r^2}{8\beta^2} - \frac{r}{8\beta^3} - \frac{tr}{2\beta G} + \frac{\tau t}{G^3} + \frac{t^2}{2G^2}\right),\\
V_{33}&\\
&= e^{r\frac{\beta}{\sqrt{\varkappa}} - \frac{Gt}{\tau}}\left[\frac{r^3}{48\beta^3} - \frac{r^2}{16\beta^4} + \frac{r}{16\beta^5} + (G^2+4\tau\beta^2)\frac{tr}{8\beta^3G^3} - \frac{tr^2}{8\beta^2G}\right.\\
&\quad \left. + \frac{t^2r}{4\beta G^2} - \frac{t^3}{6G^3} - \frac{\tau t^2}{G^4} - \frac{2\tau^2 t}{G^5}\right],\\
V_{40} &= e^{-r\frac{\beta}{\sqrt{\varkappa}} - \frac{Gt}{\tau}},\ V_{41} = e^{-r\frac{\beta}{\sqrt{\varkappa}} - \frac{Gt}{\tau}}\left(\frac{r}{2\beta} + \frac{t}{G}\right),\ V_{42}\\
&= e^{-r\frac{\beta}{\sqrt{\varkappa}} - \frac{Gt}{\tau}}\left(\frac{r^2}{8\beta^2} + \frac{r}{8\beta^3} + \frac{tr}{2\beta G} + \frac{\tau t}{G^3} + \frac{t^2}{2G^2}\right),\ V_{43}\\
&= e^{-r\frac{\beta}{\sqrt{\varkappa}} - \frac{Gt}{\tau}}\left[\frac{r^3}{48\beta^3} + \frac{r^2}{16\beta^4} + \frac{r}{16\beta^5} + (G^2+4\tau\beta^2)\frac{tr}{8\beta^3G^3} + \frac{tr^2}{8\beta^2G}\right.\\
&\quad \left. + \frac{t^2r}{4\beta G^2} + \frac{t^3}{6G^3} + \frac{\tau t^2}{G^4} + \frac{2\tau^2 t}{G^5}\right],
\end{aligned} \tag{26}$$

It is easy to show that the T-functions satisfy Eq. (23). The approximate general solution of Eq. (23), θ^b, is a linear combination of T-functions

$$\theta^b(r, t) = \sum_{n=0}^{N} c_n F_n(r, t) \tag{27}$$

where $\{F_n(r, t)\}_{n=0,1,...,N}$stands for a set of $N+1$ T-functions V_{ik}, $i = 1,2,3,4$, and $\{c_n\}_{n=0,1,...,N}$are the unknown coefficients, $c_n \in \mathbb{R}$.

The parameters $\varkappa$, τ, β, $G$and, as a consequence, $\{F_n(r, t)\}_{n=0,1,...,N}$are different for the considered regions because the thermo-physical properties of the tumor and of the surrounding tissue are assumed to be different. Therefore they all should have subscript 1 or 2. Hence, in fact, two approximate general solutions will be sought, $\theta_1^b$and θ_2^b, and two sets of unknown coefficients, $c_{ni} \in \mathbb{R}$, $i = 1,2$, in the regions $0 \le r \le R$and $R \le r \le 5R$have to be determined.

5. Inverse operator for eq. (23)

Source identification belongs to the class of inverse problems. As a rule, these problems are ill-posed and difficult to solve. To identify the spatial heat source in Eq. (8), the Trefftz method is proposed. The unknown source, Q_{r1}, is approximated by a linear combination

$$Q_{r1}(r, t) \approx \sum_{j=0}^{P} a_j b_j(r, t) \tag{28}$$

with $b_j(r, t)$, $j = 0,1, ...,P$, being monomials. If the source, $Q_{r1}$is known in the form of a function, it can be approximated using the Taylor series. The a_j, standing for unknown coefficients of the linear combination of the $b_j(r, t)$, will be found with the use of the inverse operator L^{-1}, where

$$L = \varkappa\frac{\partial^2}{\partial r^2} - \tau\frac{\partial^2}{\partial t^2} - G\frac{\partial}{\partial t} - \beta^2 \tag{29}$$

Acting on a monomial $r^k t^m$with the operator Lone obtains

$$L(r^k t^m) = k(k-1)\varkappa r^{k-2}t^m - \tau m(m-1)r^k t^{m-2} - Gmr^k t^{m-1} - \beta^2 r^k t^m \tag{30}$$

Hence, acting on both sides of (30) with the operator L^{-1}leads to a formula

$$L^{-1}(r^k t^m) = \frac{1}{\beta^2}[k(k-1)\varkappa L^{-1}(r^{k-2}t^m) - \tau m(m-1)L^{-1}(r^k t^{m-2}) - GmL^{-1}(r^k t^{m-1}) - r^k t^m] \tag{31}$$

with $L^{-1}(r^k t^m) = 0$if $k < 0$or $m < 0$. In order to find all the unknown coefficients, i.e. $a_j$and $c_{ni} \in \mathbb{R}$, $i = 1,2$, in the regions $0 \le r \le R$and $R \le r \le 5R$(comp. (27) and (28)) the objective functional that describes the mean square error of fulfilling the boundary and initial conditions, will be minimized.

For $k = 0$and $m = 0$, i.e. for a heat source of a constant efficiency, Q_m, the particular solution of Eq. (8), $\theta_2^p(r, t)$, is

$$\theta_2^p(r, t) = L^{-1}(Q_m) = -\frac{Q_m}{\beta^2} \tag{32}$$

with $Q_m = \frac{r}{\rho c}\bar{Q}_m$. It is a particular solution of Eq. (8) for $R \le r \le 5R$. The particular solution of Eq. (8) for $0 \le r \le R$, $\theta_1^p(r, t)$, can be expressed as follows:

$$\theta_1^p(r, t) = L^{-1}(Q_{r1}(r, t)) + L^{-1}(Q_{m1}) \approx \sum_{i=0}^{P} a_i L^{-1}(b_i(r, t)) - \frac{Q_{m1}}{\beta^2} \tag{33}$$

6. Heat flux expressed by temperature

Eq. (1) can be expressed as follows:

Table 1
Thermophysical properties of the tumor and the healthy tissue.

	for the tumor:	for the healthy tissue:
thermal conductivity	$\lambda_1 = 0.778$ W/(mK)	$\lambda_2 = 0.642$W/(mK)
Density	$\rho_1 = 1660$ kg/m^3	$\rho_2 = 1000$kg/m^3
specific heat	$c_1 = 2540$J/(kgK)	$c_2 = 3720$J/(kgK)
metabolic heat generation	$\bar{Q}_{m1} = 29{,}000$W/m^3	$\bar{Q}_{m2} = 450$W/m^3
relaxation time ver. 1	$\tau_1 = 14$s	$\tau_2 = 14$s
relaxation time ver. 2	$\tau_1 = 14$s	$\tau_2 = 24$s

$$\zeta + \tau\frac{\partial\zeta}{\partial t} = -\frac{\partial\left(\frac{\theta}{r}\right)}{\partial r} \tag{34}$$

$\zeta = \frac{q}{\lambda}$. Let us assume additionally that $q(r, 0) = 0$, what means that $\zeta(r, 0) = 0$. Denote the Laplace transform of a function $f(t)$as

$$\mathscr{L}[f(t)] \equiv \bar{f}(s) \tag{35}$$

Then, the Laplace transform of Eq. (34) reads

$$(1 + \tau s)\bar{\zeta} = -\frac{\partial\left(\frac{\bar{\theta}}{r}\right)}{\partial r} \tag{36}$$

$$\bar{\zeta} = -\frac{1}{1 + \tau s}\frac{\partial\left(\frac{\bar{\theta}}{r}\right)}{\partial r} \tag{37}$$

and finally, after retransforming one obtains for both regions

$$\zeta_i(r, t) = -\frac{1}{\tau_i}exp\left(-\frac{t}{\tau_i}\right)\int_0^t \frac{\partial\left(\frac{\theta_i}{r}\right)}{\partial r}(r, x)\exp\left(\frac{x}{\tau_i}\right)dx,\ i = 1,2, \tag{38}$$

7. The objective functional

The approximate solution of Eq. (8) in the region$0 \le r \le R$, $\theta_1^{ap}(r, t)$, is a sum of the general solution (27) and the particular solution (33):

$$\theta_1^{ap}(r, t) = \theta_1^b(r, t) + \theta_1^p(r, t) = \sum_{n=0}^{N} c_{n1}F_{n1}(r, t) + \sum_{i=0}^{P} a_i L^{-1}(b_i(r, t)) - \frac{Q_{m1}}{\beta_1^2} \tag{39}$$

The approximate solution of the problem in the region$R \le r \le 5R$, $\theta_2^{ap}(r, t)$, reads

$$\theta_2^{ap}(r, t) = \theta^{b2}(r, t) + \theta^{p2}(r, t) = \sum_{n=0}^{N} c_{n2}F_{n2}(r, t) - \frac{Q_{m2}}{\beta_2^2} \tag{40}$$

The objective functional, I, which describes the mean square error of fulfilling the initial, the boundary and the internal conditions, consists of two integrals:

$$I_t \equiv I_t(c_{01}, ..., c_{N1}, c_{02}, ..., c_{N2}, a_1, ..., a_P) = \int_0^{t_{end}} \{[\theta_1^{ap}(0, t)]^2 + [\theta_1^{ap}(R, t) - \theta_2^{ap}(R, t)]^2 + [\theta_2^{ap}(5R, t)]^2 + (\theta_2^{ap}(R, t) - R(T_{cr} - T_b)g(\Phi, t))^2 + [\lambda_1\zeta_1(R, t) - \lambda_2\zeta_{12}(R, t)]^2\}dt$$

$$I_r \equiv I_r(c_{01}, ..., c_{N1}, c_{02}, ..., c_{N2}, a_1, ..., a_P) = \int_0^R \left\{[\theta_1^{ap}(r, 0)]^2 + \left[\frac{\partial\theta_1^{ap}}{\partial t}(r, 0)\right]^2\right\}dr + \int_R^{5R} \left\{[\theta_2^{ap}(r, 0)]^2 + \left[\frac{\partial\theta_2^{ap}}{\partial t}(r, 0)\right]^2\right\}dr$$

Hence

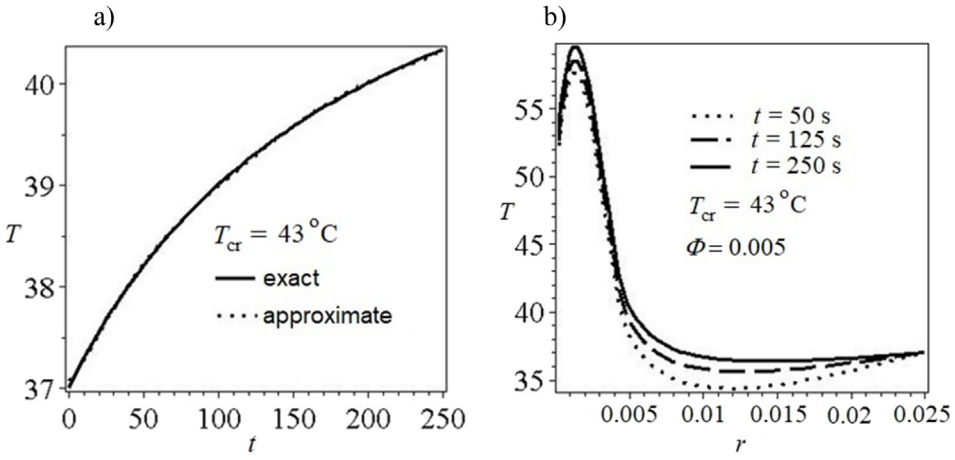

Fig. 1. a) The anticipated exact and approximate temperature for $r = R$. b) The temperature distribution in the entire area for selected moments of time. Calculations for $\tau_1 = \tau_2 = 14$s. Identified heat source intensity $\bar{Q}_{r1} = 3.18{\cdot}10^7 \mathrm{W/m^3}$.

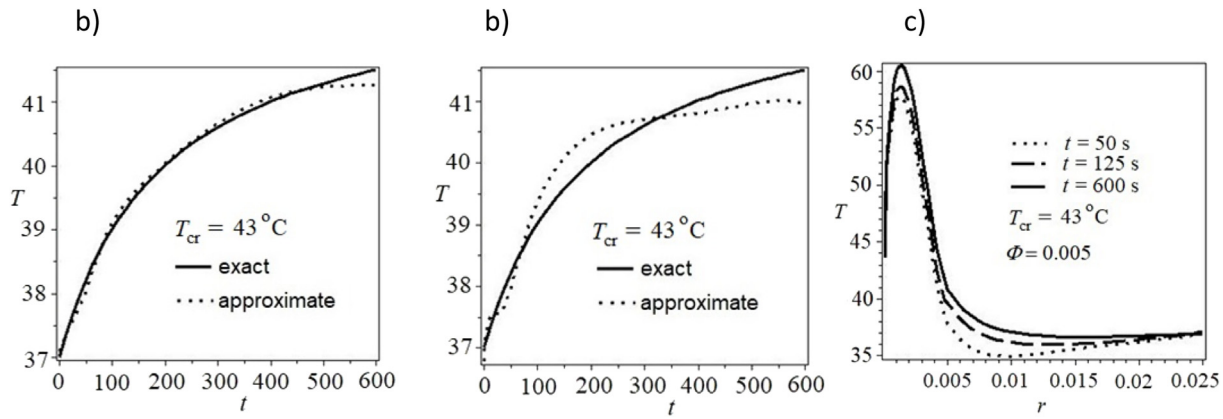

Fig. 2. The anticipated exact and approximate temperature for $r = R$a) in the tumor, b) inthe healthy tissue. c) The temperature distribution in the entire area for selected moments of time. $\tau_1 = \tau_2 = 14$s. Identified heat source intensity $\bar{Q}_{r1} = 3.18{\cdot}10^7 \mathrm{W/m^3}$.

$$I(c_{01},\ldots,c_{N1},\ c_{02},\ldots,c_{N2},\ a_1,\ldots,a_P) = I_t + I_r \tag{41}$$

Minimizing the objective functional with respect to the indicated coefficients and next the substitution

$$T = \begin{cases} T_b + \frac{1}{r}\theta & \text{for} \quad r > 0 \\ T_b + \frac{\partial \theta_1}{\partial r} & \text{for} \quad r = 0 \end{cases} \text{and } q = \lambda\zeta \tag{42}$$

leads to the solution of the considered problems.

8. Results and discussions

The presented results are obtained for a small spherical tumor of a radius $R = 0.005$m embedded in a surrounding muscle tissue. The values of the thermophysical properties, (Andra et al., 1999, LiuLin C, 2010), are presented in Table 1.

Regarding the time of relaxation, the first version was assumed to be the same in the tumor and in healthy tissue. Since Kaminski, 1990, reported that in a healthy biological tissue the relaxation time can be 20–30 s and more, in the second version adopted $\tau_2 = 24$s was taken to check whether the relaxation time can dominate the behavior of thermal wave propagation. The corresponding perfusion rates and the volumetric heat capacity of blood for both the tumor and the surrounding healthy tissue, are as follows: $w_{b1} = w_{b2} = 0.0064\mathrm{m^3/s/m^3}$, $\rho_b c_b = 4.18{\cdot}10^6 \mathrm{J/m^3/K}$, (Bagaria and Johnson, 2005). The blood temperature is assumed to be $T_b = 37$°C. For the critical temperature two variants are considered: a) $T_{cr} = 43$°C, b) $T_{cr} = 45$°C.

Three kinds of the unknown heat source, Q_{r1}, were considered:

a) linear with respect to space variable, $Q_{r1}(r) = Q_{r1}\left(1 - \frac{r}{R}\right)$,
b) Gaussian distribution of heat, $Q_{r1}(r) = Q_{r1} exp\left(-\frac{r^2}{(0.5R)^2}\right)$,
c) two kinds of polynomial form of the heat source in the tumor, $Q_{r1}(r, t) = q_0 + q_1 r + q_2 t$and $Q_{r1}(t) = q_0 + q_1 t$.

Of course, in the case a) and b) the substitution (7) holds, i.e. $Q_r = \frac{r}{\rho c}\bar{Q}_r$.

Since the anticipated temperature is assumed to be equal to $R(T_{cr} - T_b)g(\Phi, t)$, forg$(\Phi, t)$, two different functions have been considered:

a) $g(\Phi, t) = \frac{\Phi t}{1 + \Phi t}$for Φ=0.005, 0.01, 0.015 ;
b) $g(\Phi, t) = 0.004t$for $t \in (0,\ 250)$;

The most satisfactory results were obtained for case a). Case b) , i.e. linear change of temperature in time for $r = R$, gave a bit less satisfactory results.

To identify the heat source, a different number of T-functions was used. However, for all of them the intensity of the heat source was almost the same. Finally, only 20 T-functions were used in linear combination, (27), because for such number of T-functions the temperature field, calculated as a verification of the results obtained for the heat source intensity, was approximate enough. The anticipated temperature change for $r = R$was used with $\Phi = 0.005$and $T_{cr} = 43$°C. On the first four Figures the spatial heat source was assumed in the shape of a triangle, i.e. $Q_{r1}(r) = Q_{r1}{\cdot}\left(1 - \frac{r}{R}\right)$, where intensity of the source

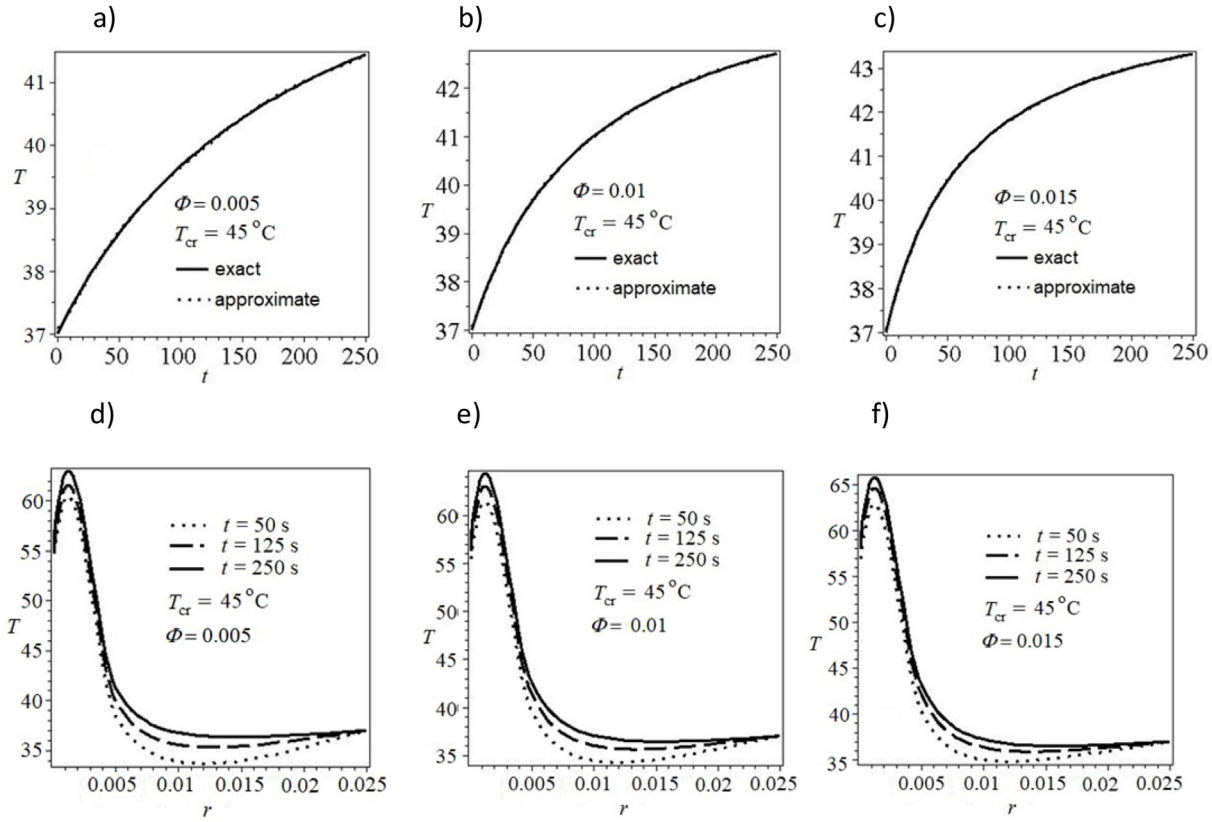

Fig. 3. The anticipated exact (according to $g(\Phi, t) = \frac{\Phi t}{1+\Phi t}$) and approximate temperature for $r = R$(charts a), b) and c)) and the temperature distribution. (charts d), e) and f)). $\tau_1 = \tau_2 = 14$s.

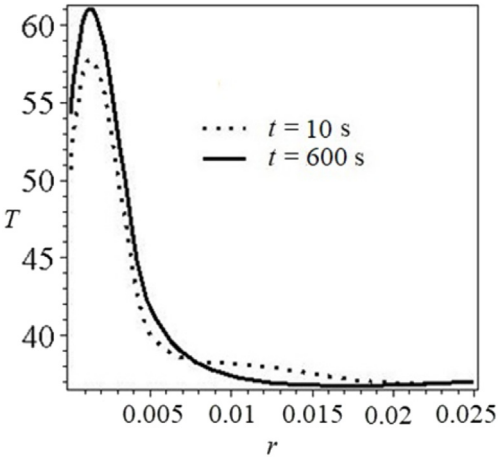

Fig. 4. Approximate solution of the direct problem for $\bar{Q}_{r1} = 3.18{\cdot}10^7$W/m^3 and conditions (10) to (15). $\tau_1 = \tau_2 = 14$s.

$\bar{Q}_{r1}$should be determined. Using formula (31), the particular solution is calculated as $Q_{r1}{\cdot}(L^{-1}(1) - L^{-1}(r)/R)$. Fig. 1 presents an approximation of the anticipated condition for $r = R$according to $g(\Phi, t) = \frac{\Phi t}{1+\Phi t}$, $\Phi = 0.005$(practically the same approximation in both regions) and the resulting temperature changes with respect to r for three selected moments of time for $t \in (0,\ 250)$s. The calculated intensity of the heat source was $\bar{Q}_{r1} = 3.18{\cdot}10^7$W/m^3. Inaccuracies of the temperature field in the vicinity of $r = 0$are the result of the low number of T-functions. This is repeated on all temperature charts, but it is enough to state their physical nature.

For $t \in (0,\ 600)$s the predicted temperature for $r = R$, denoted in Fig. 2a and b as "exact" is not approximated in the same way for $0 < r < R$and $R < r < 5R$. Thus for $r = R$the temperature distributions calculated for the tumor according to Eq. (8) for $i = 1$(Fig. 2a) and for the healthy tissue according to Eq. (8) for $i = 2$(Fig. 2b) are slightly different. The obtained heat source intensity has the same value as the one obtained for $t \in (0,\ 250)$s, Fig. 1.

However, in both cases the temperatures $T(R,\ 250) = 40.3$°C and $T(R,\ 600) = 41.2$°C are lower than 42,5°C. Therefore, the calculations for $T_{cr} = 45$°C and for Φ=0.005, 0.01, 0.015 were carried out. The results are shown in Fig. 3. For all three values of $\Phi$the approximations of the anticipated condition for $r = R$were practically the same in both regions, but the maximal temperature achieved for $t = 250$s was different. Values of the identified heat source identity for the three values of Φwere equal to, respectively, $3.29{\cdot}10^7$, $3.31{\cdot}10^7$and $3.34{\cdot}10^7$W/m^3. In these cases, the temperature $T(R,\ 250)$is equal to 41.4, 42.7 and 43.3 °C, respectively. It means that for the triangular heat source the heat source intensity should be equal to at least $3.30{\cdot}10^7$W/m^3 or greater. It is also important that the temperature of the healthy tissue should be about 37 °C.

The final verification of the correctness of the calculations are the results of the initial boundary (direct) problem, where the temperature for $r = R$is not anticipated, and the intensity of the spatial triangular heat source is imposed. Fig. 4 presents the temperature distribution in the moments of time (initial and final) obtained for $\bar{Q}_{r1} = 3.18{\cdot}10^7$W/m^3 and initial and boundary conditions (10) to (15). For these intensity of the heat source $T(R,\ 250) = 41.8$°C, which confirms the previous observation that the heat source intensity should be equal to at least $3.30{\cdot}10^7$W/m^3. The temperatures in the tumor are sufficient to kill cancer cells. Of course, the changes of temperature in time for $r = R$are different than those anticipated in the inverse problem, because in this calculation it is not imposed.

On the next three Figures the Gaussian distribution of heat in the tumor was assumed, i.e. $Q_{r1}(r) = \bar{Q}_{r1}{\cdot}exp\left(-\frac{r^2}{(0.5R)^2}\right)$,where intensity $\bar{Q}_{r1}$of

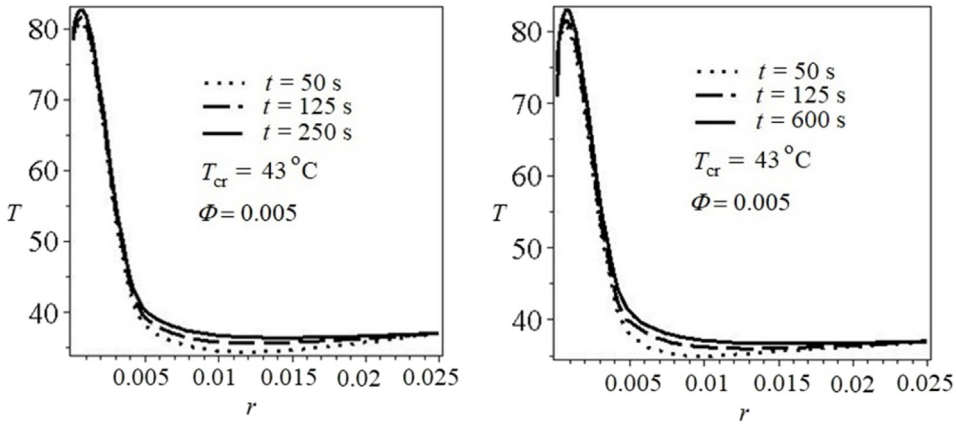

Fig. 5. Temperature distribution in the tumor and the healthy cells for a) $t \in (0,\ 250)$s b) $t \in (0,\ 600)$ s. $\bar{Q}_{r1} = 5.06 \cdot 10^7 \mathrm{W/m^3}$. $\tau_1 = \tau_2 = 14$s.

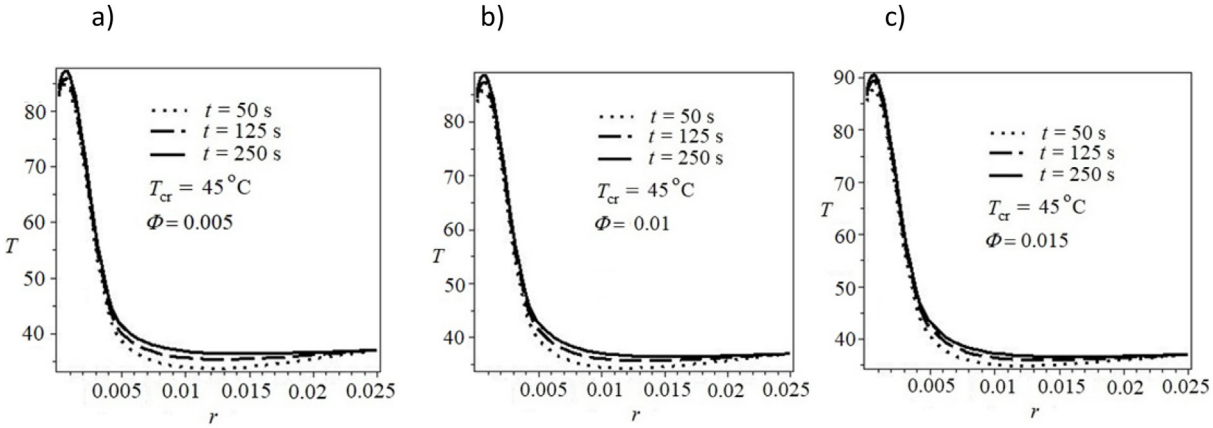

Fig. 6. Temperature distribution in the tumor and the healthy cells for $\Phi = a)$ 0.005, b) 0.01, c) 0.015 and for $T_{cr} = 45^{\circ}$C. $\tau_1 = \tau_2 = 14$ s.

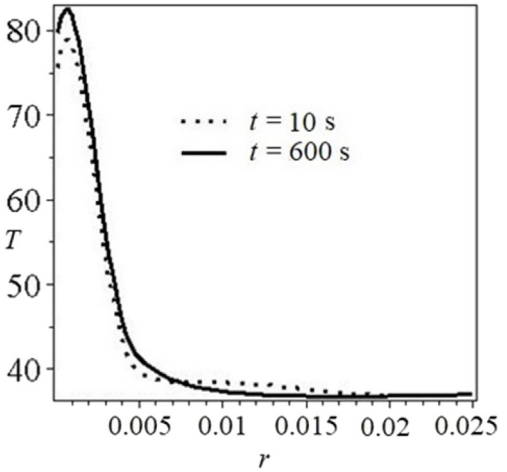

Fig. 7. Approximate solution of the direct problem for $\bar{Q}_{r1} = 5 \cdot 10^7 \mathrm{W/m^3}$ and conditions (10) to (15). $\tau_1 = \tau_2 = 14$s.

the source should be determined. To get the particular solution the term $exp\left(-\frac{r^2}{(0.5R)^2}\right)$is expanded into Taylor series. Next, thanks to formula (31) the inverse operator for monomials can be calculated. In the calculations below, 50 terms of the expansion have been taken into account. Fig. 5 presents temperature distribution for $0 \le r \le 5R$for $t \in (0,\ 250)$s and for $t \in (0,\ 600)$s. In both time intervals the calculated heat source intensity is $\bar{Q}_{r1} = 5.06 \cdot 10^7 \mathrm{W/m^3}$. Approximation of the anticipated temperature is exactly the same as for the triangular heat source identified in these intervals.

In both cases presented in Fig. 5 the temperatures $T(R,\ 250) = 41.3^{\circ}$C and $T(R,\ 600) = 41.0^{\circ}$C are lower than 42,5°C. Therefore, the calculations for $T_{cr} = 45^{\circ}$C and for Φ=0.005, 0.01, 0.015 were carried out again. Approximation of the anticipated temperatures for $r = R$is the same as shown in Fig. 3a, b and 3c, respectively. Hence, the temperature $T(R,\ 250)$is equal to 40.3, 42.7 and 42.7 °C, respectively. Values of the identified heat source intensity for the three values of Φwere equal, respectively, $5.25 \cdot 10^7$, $5.26 \cdot 10^7$and $5.33 \cdot 10^7 \mathrm{W/m^3}$. It means that for the Gaussian distribution of heat in the tumor the heat source intensity should be equal to at least $5{,}3 \cdot 10^7 \mathrm{W/m^3}$ or greater, while the temperature of the healthy tissue is about 37 °C. The results are shown in Fig. 6.

Approximate solution of the direct problem for the Gaussian distribution of heat, which verifies the obtained results, obtained for $\bar{Q}_{r1} = 5 \cdot 10^7 \mathrm{W/m^3}$ and initial and boundary conditions (10) to (15), is presented in Fig. 7. Again, it confirms the previous observation that the heat source intensity should be equal to at least $5.3 \cdot 10^7 \mathrm{W/m^3}$. The temperatures in the tumor are sufficient to kill cancer cells and the changes of temperature in time for $r = R$are different from those anticipated in the inverse problem.

For both shapes of the spatial heat source in the tumor the calculations were also led for $\tau_1 = 14$sand $\tau_2 = 24$s and $T_{cr} = 45^{\circ}$C with anticipate temperature for $r = R$as in the previous cases. The obtained values of the intensity of the heat source differ slightly from those calculated in the cases shown in Fig. 3a for the triangular shape and in Fig. 5 for the Gaussian shape of the spatial heat source and are equal to $3.22 \cdot 10^7$and $5.12 \cdot 10^7\ \mathrm{W/m^3}$, respectively. The temperature distribution is presented in Fig. 8.

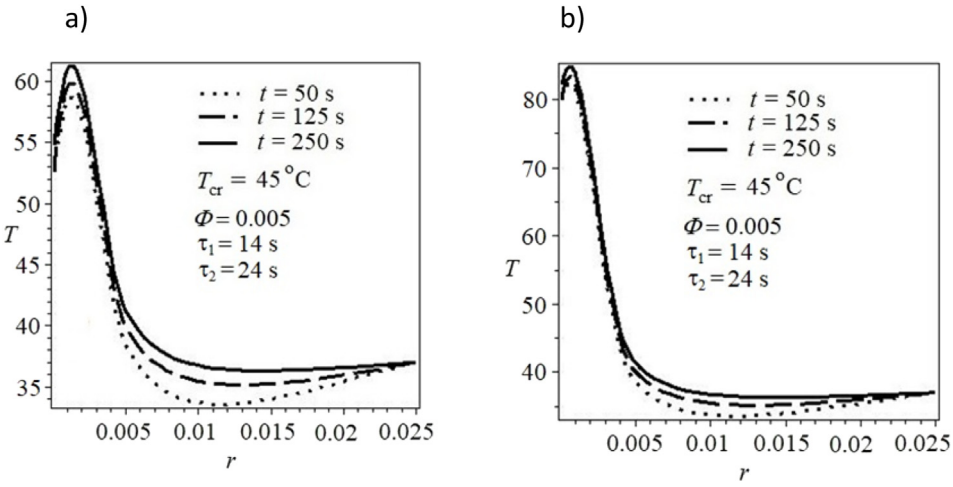

Fig. 8. Temperature distribution in the tumor and in the healthy cells for $\Phi = 0.005$, $T_{cr} = 45^{o}$C. $\tau_1 = 14$s and $\tau_2 = 24$s for a) triangular, b) Gaussian shape of the heat source.

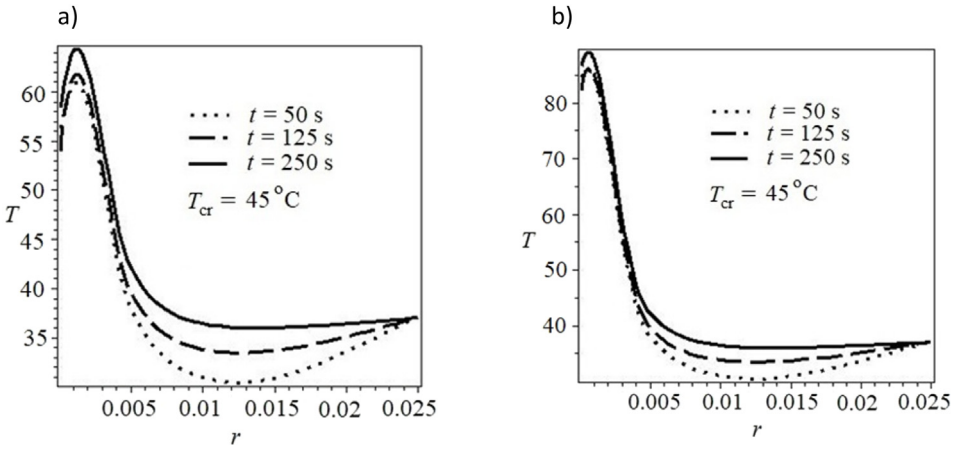

Fig. 9. Temperature distribution in the tumor and in the healthy tissue for $T_{cr} = 45^{o}$C. $\tau_1 = \tau_2 = 14$s for a) triangular, b) Gaussian shape of the heat source.

In both cases presented in Fig. 8 the temperature $T(R,\ 250) = 41.4^{o}$C is lower than 42.5°C. The temperature presented in Fig. 8a is similar to that presented in Fig. 3d; a similar situation occurs with Figs. 8b and 6a. It follows that different relaxation times do not affect the determination of the intensity of the heat source in a fundamental way. This means that increasing relaxation time in healthy tissue from 14 s to 24 s has little effect on the behavior of thermal wave propagation.

The polynomial form of the heat source being identified in the tumor, $Q_{r1}(r,\ t) = q_0 + q_1 r + q_2 t$and $Q_{r1}(t) = q_0 + q_1 t$gave results with intensity of the heat source $Q_{r1}(r,\ t) = 24895.1 + 2.16r + 5.83t$and $Q_{r1}(t) = 32176.9 + 0.8876t$, respectively. In both cases the expression $q_0$has a value of two orders of magnitude lower than in previous cases of heat sources. Since with the assumed triangular form of the heat source as well as with its Gaussian form the intensities of the heat source obtained were of the order of 10^7W/m^3, the assumption about the polynomial form of the identified source of heat, as presented in point c) when discussing the anticipated form of these intensities at the beginning of this section, should be regarded as erroneous. This conclusion is confirmed by the results presented by LiuLin C, 2010, where the intensity of heat source equal to 6.15·106 W/m^3 is reported for the case when the tumor was heated up to about 5.7° above 37 °C. However, they considered a tumor with a radius of 0.00315 m, i.e. much smaller than that considered in this paper.

Finally, the case when the anticipated temperature was assumed in the form $R(T_{cr} - T_b)g(\Phi,\ t)$for $t \in (0,\ 250)$was considered for $T_{cr} = 45^{o}$C and $\tau_1 = \tau_2 = 14$s. The results for the triangular as well as for the Gaussian shape of heat source are presented in Fig. 9. It is worth mentioning that $T(R,\ 250) = 42.3^{o}$C. The anticipated temperature is approximated with a very good accuracy. The intensity of the sources is $3.33{\cdot}10^7$W/m^3 for the triangular source and $5.31{\cdot}10^7$W/m^3 for the Gaussian distribution of heat. The results are similar to those obtained for the anticipated temperature $R(T_{cr} - T_b)\frac{\Phi t}{1+\Phi t}$for Φ=0.015.

For both cases, the triangular heat source and Gaussian distribution of heat, the identified intensity of heat source was of the order of 10^7 W/m^3. Moroz et al., 2002, stated that magnetic fluid hyperthermia has the maximum potential for destroying tumor cells and that magnetic particles injected into the center of tumor diffuse in the Gaussian distribution. Hence, considering the identified intensity of heat sources one comes to the conclusion that the results obtained for the Gaussian distribution of heat are the most valuable. Therefore, for the considered tumor, one can assume value 5.3 to $5.4{\cdot}10^7$W/m^3 as the value of spatial heat source intensity.

LiuLin C, 2010 considered heating a tumor of a radius 0.00315 m, and for intensity of the spatial heat source with Gaussian distribution, arrived to the value $6.15{\cdot}10^6$W/m^3 for $Q_{r1}(r) = Q_{r1}exp\left(-\frac{r^2}{(\varphi R)^2}\right)$with $\varphi = 0.04$. They came to the conclusion that when $\varphi$is increased, the heating conditions are improved. Comparing their results with the results in this article, it can be concluded that they are consistent.

9. Conclusions

The Trefftz method has been used to identify the intensity of spatial heat source in the hyperthermia of a tumor. The inverse problem for the non-Fourier bio-heat equation with a space-dependent source term in a spherical coordinate system has been solved. Correctness of the results for both triangular and Gaussian spatial heat sources has been verified by means of solving the initial boundary (direct) problem, where the temperature for $r = R$is not anticipated, and the intensity of the spatial triangular heat source is imposed. The influence of the spatial heat source's shape and of the type of anticipated temperature on the border of the tumor and the healthy tissues is considered and discussed. The results show that the intensity of the heat source described by the triangular function (case a) shown at the beginning of the previous section leads to a 20 °C lower temperature than the case of the Gaussian function (case b). Also, the intensity of the heat source is lower in this case.

The change of blood perfusion rate has not been investigated. However, LiuLin C, 2010, claim that blood perfusion may play the cooling role, while the temperature of blood is assumed to have a constant value of 37 °C.Change of the relaxation time in the tissue is of minor importance. Since in the considered cases the speed of the thermal signal is of the order of 0.0001 m/s, the intensity of the spatial heat source has to be high so as to warm the tumor up to the temperature in which the cancer cells die.

The calculations have been carried out using the Maple software. It is widely known that the Trefftz method leads to a bad-conditioned matrix of linear system of equations. This software enables to use symbolic calculations which avoid problems with the rounding error. Moreover, Maple enables generating Trefftz functions in a very easy way.

References

Andra, W., d'Ambly, C.G., Hergt, R., Hilger, I., Kaiser, W.A., 1999. Temperature distribution as function of time around a small spherical heat source of local magnetic hyperthermia. J. Magn. Magn. Mater. 194, 197–203.

Bagaria, H.G., Johnson, D.T., 2005. Transient solution to the bioheat equation and optimization for magnetic fluid hyperthermia treatment. Int. J. Hyperth. 21, 57–75.

Cattaneo, C., 1958. Sur une forme de l'equation de la chaleur elinant le paradoxes d'une propagation instantance. C. R. Acad. Sci. 247, 431–432.

Ciałkowski, M.J., Grysa, K., 2010. Trefftz method in solving the inverse problems. J. Inverse Ill-Posed Probl. 18 (6), 595–616.

Field, S.B., 1987. Hyperthermia in the treatment of cancer. Phys. Med. Biol. 32 (7), 789–811.

Fu, Z.J., Xi, Q., Ling, L., Cao, C.Y., 2017. Numerical investigation on the effect of tumor on the thermal behavior inside the skin tissue. Int. J. Heat Mass Transf. 108, 1154–1163.

Grysa, K., Maciąg, A., Adamczyk-Krasa, J., 2014. Trefftz functions applied to direct and inverse non-fourier heat conduction problems. J. of Heat Transfer - Trans. of the ASME 136 (9) 091302-1 - 091302-9.

Grysa, K., 2010. Trefftz Functions and Their Applications in Solving the Inverse Problems. Kielce University of Technology Publishers, Kielce, Poland (in Polish).

Habash, R.W.Y., Bansal, R., Krewski, D., Alhafid, H.T., 2006. Thermal therapy, Part 2:hyperthermia techniques. Crit. Rev. Biomed. Eng. 34 (6), 491–542.

Hafid, M., Lacroix, M., 2017. An inverse heat transfer algorithm for predicting the thermal properties of tumors during cryosurgery. International Journal of Biomedical and Biological Engineering 11 (6), 352–360.

Hall, E.J., Roizin-Towle, L., 1984. Biological effects of heat. Cancer Res. 44, 4708s–4713s.

Kaminski, W., 1990. Hyperbolic heat conduction equation for materials with a non-homogenous inner structure. ASME J. Heat Transfer 112, 555–560.

Khanday, M.A., Aijaz, M., Rafiq, A., 2013. Mathematical analysis on the treatment of cancerous tumors using therapy based on local hyperthermia. Journal of Energy, Heat and Mass Transfer 35, 295–305.

Kołodziej, J., Zieliński, A.P., 2009. Boundary Collocation Techniques and Their Application in Engineering. WIT Press, Southampton, UK.

Li, Z.C., Lu, T.T., Hu, H.Y., Cheng, A.H.D., 2008. The Trefftz and Collocation Methods WIT Press, Southampton, UK.

Liu, C.S., Kuo, C.L., Jhao, W.S., 2016. The multiple-scale polynomial Trefftz method for solving inverse heat conduction problems. Int. J. Heat Mass Transf. 95, 936–943.

Liu, K.C., 2007a. Analysis of thermal behavior in multi-layer metal thin-films based on hyperbolic two-step model. Int. J. Heat Mass Transf. 50, 1397–1407.

Liu, K.C., 2007b. Numerical analysis of dual-phase-lag heat transfer in a layered cylinder with nonlinear interface boundary conditions. Comput. Phys. Commun. 177, 307–314.

Liu, K.C., 2008. Thermal propagation analysis for living tissue with surface heating. Int. J. Therm. Sci. 47, 507–513.

Liu, K.C., Lin, C.N., 2010. Temperature prediction for tumor hyperthermia with the behavior of thermal wave, numerical heat transfer, Part A: applications. Int. J. Comput. Methods 58 (10), 819–833.

Luna, J.M., Guerrero, A.H., Méndez, R.R., Ortiz, J.L.L., 2014. Solution of the inverse bio-heat transfer problem for a simplified dermatological application: case of skin cancer. Ingeniería Mecánica Tecnología y Desarrollo 4 (6), 219–228.

Maenosono, S., Saita, S., 2006. Theoretical assessment of FePt nanoparticles as heating elements for magnetic hyperthermia. IEEE Trans. Magn. 42, 1638–1642.

Moroz, P., Jones, S.K., Gray, B.N., 2002. Magnetically mediated hyperthermia: current status and future directions. Int. J. Hyperth. 18, 267–284.

Rojczyk, M., Orlande, H.R.B., Colac, M.J., Szczygieł, I., Nowak, A.J., Białecki, R.A., Ostrowski, Z., 2015. Inverse heat transfer problems: an application to bioheat transfer. Comput. Assist. Mech. Eng. Sci. 22, 365–383.

Siegel, R., Naishadham, D., Jemal, A., 2013. Cancer statistics. A Cancer J Clin 63, 11–30.

Soltani, M., Chen, P., 2012. Effect of tumor shape and size on drug delivery to solid tumors. J. Biol. Eng. 6, 4.

Vernotte, P., 1958. La veritable equation de la chaleur. C. R. Acad. Sci. 247, 2103–2105.

Weymann, H.D., 1967. Finite speed of propagation in heat conduction, diffusion and viscous shear motion. Am. J. Phys. 35 (6), 488–496.